# A global method of generating action potentials and EEG oscillations in a topological surface network

## Model Predictions and Speculations

Siddhartha Sen (Email: sen1941@gmail.com)
*Centre for Research in Adaptive Nanostructures and Nanodevices,*
*School of Physics, Trinity College Dublin, Ireland*

## Acknowledgment

I would like to thank Samik Sen for producing all the EEG waveform Gnuplots. Mike Coey, for encouragement, Tomas Ryan and Maurizio Pezzoli for numerous discussions, and David Muldowney for reading through and commenting on an earlier version of this work. This research did not receive any specific grant from funding agencies in the public, commercial or not-for-profit sector.

## Abstract

In this paper we show how both action potential-like soliton pulses and EEG-like waveform surface excitations can be generated by exploiting the topological connectivity properties of a hypothetical brain connectome, in a surface network, which we prove, exactly captures the topological architecture of any hypothetical brain connectome. This network, it is shown, can generate a wide variety of one dimensional action potential like soliton voltage pulses and soliton generation co-produce two dimension surface waveforms provided the network is charged and has surface spin half particles on it. Both soliton pulses and the co-produced surface waveforms are generated in the network in responds to local pinch surface deformations input signals, that produce signals exploiting the system's topology. The analytic expressions and oscillation frequencies of the surface waveforms are determined. It is found that the frequencies are inversely relate to amplitudes and that the surface waveforms correspond to the symmetric tiling of a spherical surface. Greens function methods for studying how the waveforms are modulated by other signals are established and are used to explain a complex sequence of surface excitations observed in deep sleep. In an earlier paper it was shown that the charged soliton pulses carry details of the input deformation parameters that create them and transfer this information to the pathways they traverse, as a helical non-transient topologically stable magnetic alignment of surface spins: a memory substrate, with a natural, theoretically determined, excitation frequency range. It is shown how sleep spindles observed in deep sleep, may reflect the presence of these memory excitation frequencies and that soliton pulses and surface waveforms might cooperate to retrieve memory, identify incoming signals and help focus attention.

keywords: memory retrieval, solitons , transient excitations, surface waveforms, K-complexes, sleep-spindles, sharp-wave ripples, attention.

## Introduction

In this paper we complete a project to demonstrate that it is possible to produce all observed brain excitations in a special topological surface network that exactly captures the complex topological connectivity properties of a brain connectome. Such a scheme has predictive powers. We prove that such a network exists by using the mathematical theorem on the topological classification of surfaces,(Munkres,2014) and then show how both one dimensional action potential like soliton voltage pulses as well as surface EEG like waveforms can be generated in it by global means: thus linking its form to its function. In an earlier paper (Sen,2021)it was shown that action potential like one dimensional soliton voltage pulse excitations, that carry a topological charge, could be created from such in a surface network in response to local pinch deformations that produced signals that are dependent on the topology of the network, provided the network was charged and had surface spin half particles. These surface spins $s_i, i = 1, 2$ are described by two components, have magnetic properties and give the surface a new topological feature, namely, a spin structure. This means that the surface spins can be arranged in topologically distinct patterns which cannot be continuously deformed into each other. Thus if we intuitively think of surface spin as arrows on the surface then an aligned linked array of spins going round a tube of the network in the clockwise direction is topologically different from an array going round in the anticlockwise direction as the two arrangements cannot be related by continuous deformations.

We show how the topological process of creating soliton pulse excitations also co-produce surface waveforms with EEG waveform like properties and it is possible to directly link the form of an EEG waveform co-produced by a soliton from its topological charge. The argument given is of a general natureand is followed by the determination of the detailed properties of these EEG waveforms and the development of mathematical tools to study how these waveforms are modulated by other signals. The results obtained are predictions. There are no ad hoc features present in the approach. All the results obtained follow from requiring that both input signals as well as the surface network's response to them respect the mathematical properties of surface introduced. This is the dynamical hypothesis that defines the surface network. We will identify the soliton excitations found as action potentials on the network and the surface oscillations they co-produce as EEG waveforms.

The importance of topology(Nash,1983;Bassett,2020) for exploring global features of the brain is now beginning to be recognized in neuroscience and elsewhere. Topology is the mathematical discipline that studies spaces and structures that do not change under continuous deformations. For example a line and a circle are topologically different but a circle and a square or a triangle are the same. Topological structures are robust. They are global properties of a system. For this reason there is growing interest in using topological methods to identify hidden robust structures present in the vast amount of data available that describe the connectivity architecture of the brain's axon network. This is an important area of current research. Another area of exploration where topological and algebraic geometry methods are being used is to unravel the information contained in brain signals. A few representative references in these growing areas of research are: (Bassett,2020; Curto,2017; Reimann,2017; K.Hess, 2018; M.Marcolli,2019).

In the spirit of searching for global ways of understanding the functioning of the brain, we prove that, remarkably, it is possible to construct a special surface network that exactly captures the topological connectivity architecture of any hypothetical brain connectome and show (Sen,2021) that this surface network can generate action potential-like soliton excitations, by local input signals represented by local surface deformations. The scheme proposed differs significantly from existing methods of signal generation, (Scott,2002; Heimburg,2005; Shrivastava,2020) in two important ways: signals are generated by global means where the topology of the surface network and the presence of surface spin half particles play an essential role, and the soliton pulses generated carry with them the surface deformation information that create them. It was shown how the soliton signals can transfer this information to the pathways they traverse leaving a non-transient topologically stable helical magnetic structure: a memory substrate. The structure is produced by the alignment of surface spin half particles by their interaction with the transient helical magnetic field produced when charged soliton signals move through the network. The structure is held together by spin-spin interactions and is stable due to its topological form. It is a periodic structure with a natural excitation frequency that was theoretically determined to be in the range $(1 - 30+)$ Hz (Sen,2021). This suggests that memories, stored in this way, may be retrieved by oscillating electromagnetic signals either external or internally generated that have frequencies that overlap with memory label frequencies. Memory retrieval, in the scheme, is by a resonance excitation mechanism.

We now summarize three important features of the scheme(Sen,2021): we prove that there is a special surface. which we choose for as our surface network, called a Riemann surface, that exactly capture the topological architecture of a brain connectome, we then justify using pinch deformations as input signals and finally we explain how the surface network produces one dimensional action potential-like soliton voltage pulses that are solutions of the non-linear Schroedinger differential equation. With these results in place we move on to show how EEG-like waveforms are naturally co-produced in the scheme, whenever soliton signals are created and establish their properties.

We can think of a Riemann surface as a ubersurface covering the brain's assembly of three dimensional neurons. This is shown in Fig 3.

We now prove that it is possible to find a smooth mathematical surface network that exactly captures the topological architecture of a hypothetical connectome of the brain. Consider a hypothetical connectome. Next cover it by a smooth surface. This creates a very complex two dimensional smooth surface with a complex array of thin tubes joined together in different surface regions. As we do not know the details of the connectome the complex connectivity

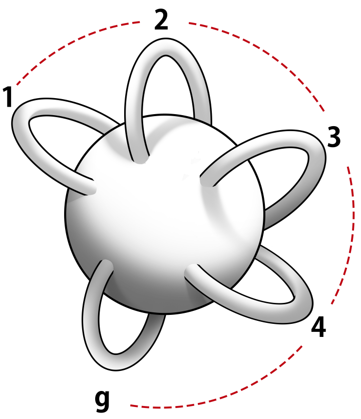

**Fig. 1** Genus $g$ surface

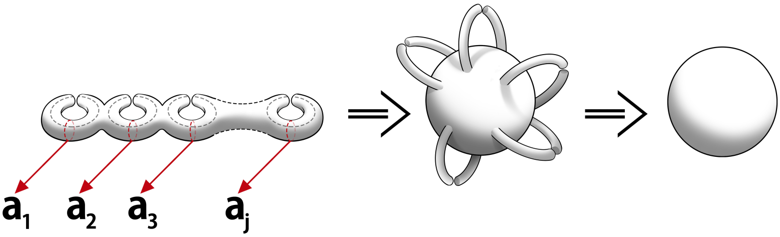

**Fig. 2** Degenerate Riemann Surface due to pinching

of this surface is also unknown. But at this point we make use of a remarkable theorem on the topological classification of surfaces, (Munkres,2014). The theorem tells us that no matter how complex and intricate are the unknown connection details of the underlying connectome the surrounding surface, is topologically equivalent to a sphere with tubes (Fig1) or an orderly array of donut surfaces Fig 3. The unknown connectivity details show up in the unknown number of loops on the sphere or the unknown number of donut surfaces present. The theorem tells us that this surface can be represented in many different ways.Thus the same topologically connected surfaces can be represented in the form of Fig1 or Fig 3. The smooth topological surface produced is known as a Riemann surface. We will call this mathematical Riemann surface an “ubersurface” as it can viewed as a mathematical surface that covers the brain’s assembly of three dimensional individual linked neurons. If we stick to the donut picture we note that the unknown, but large number of donuts $g$ present, in the ubersurface is called the genus of the Riemann surface. Donut joined together, as shown in Fig 3, have genus values $g \geq 1$. The surfaces with $g = 0$ is a sphere. It is related to a genus $g$ by pinch deformations as shown in Fig 2.

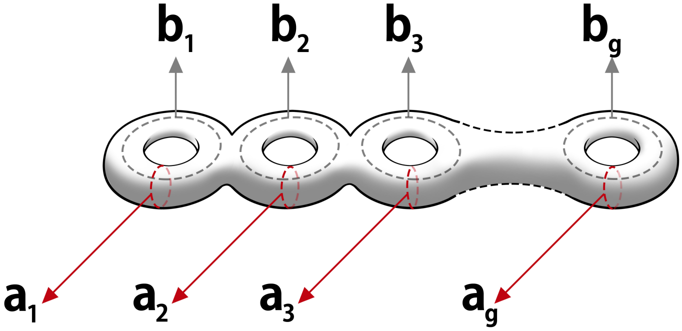

**Fig. 3** Marked Riemann.

There are many possible smooth non-equivalent mathematical Riemann surfaces with spin structure that can capture the brain's intricate connectivity architecture. But within this class, it can be proved (Arbarrello,2001), that there is a special subclass that can generate the wide variety of brain-like signals by local surface deformations provided the special surfaces is charged and has a spin structure. It also has a modular structure which means it contains a large number of connected subunits. The details of this special surface are discussed in Sen(Sen,2021).

The next step is to introduce input signals. An input signal on the surface will be taken to be a local set of surface deformations that are consistent with the mathematical features of the ubersurface and it is required that the response of the surface to these deformations produces action potential like soliton signals. This is the case. Surprisingly the response signals can be shown to be one dimensional multi-soliton solutions of the non-linear Schroedinger equation. This fact justifies choosing local pinch deformation that locally reduce the circumference of a network tube to zero (Fig 2) as input signals. A pinch deformation can be produced in many different ways. They can be produced by mechanical, electrical, chemical or gas inputs.

Let us next explain how solutions of the non-linear Schroedinger equation appear from the qualitative geometrical picture described. To do this we need two mathematical results. The first result is that a charged Riemann surface with spin structure can also be described by an algebraic function called the Riemann theta function where its variables are constructed from the topological coordinate variables of the Riemann surface and the spin structure of the Riemann surface is captured by a set of discrete variables called characteristics (Sen,2021). The second is that the algebraic Riemann theta function describes a Riemann surface only if it satisfies a nonlinear identity called the Fay trisecant identity.(Mumford,1987). To proceed we need to briefly describe the variables used to describe a Riemann surface and those used to define its associated Riemann theta function.

In this paper no further details about Riemann surfaces or the Riemann theta function are required. The information about the variables used to define both a Riemann surface and its associate Riemann theta function, which we now sketch, is all that is required to understand the global method of signal generation described. Details of these mathematical objects are given in Mumford (Mumford,1987).

For a genus $g$ Riemann surface the topological coordinates are, $2g$ loop coordinates $(a_i, b_i), i = 1, 2, ..g$ shown in Fig 3, that capture the topological connectivity properties of the Riemann surface and $g$ smooth one forms $\omega_i(z)dz, i = 1, 2, ..g$, where $z$ is a complex variable that represents a point on the Riemann surface. The set of one forms capture the smoothness of the Riemann surface. The one forms are normalized by requiring $\int_{a_i} du\omega_j(u) = \delta_{ij}$ where $\delta_{ij} = 0, i \neq j; = 1, i = j$, and the integral is a closed circuit along the loop coordinate $a_i$, surface spins are represented by spin fields $s_i(z), i = 1, 2$. The corresponding algebraic Riemann theta function has variables that are constructed from the topological coordinates of the Riemann surface. They are $g$ complex variables $z_i, i = 1, 2, ..g$ constructed from one one complex variable $z$ that represents a point on the Riemann surface by the map $z_i = \int_0^z du\omega_i(u), i = 1, 2, ..g$ and the symmetric complex valued matrix $\Omega_{ij} = \int b_j du\omega_i(u)$, where the integral is round a loop $b_j$, while the spins $s_i(z), i = 1, 2$ on the Riemann surface are now represented by a set of $2g$ variables $(\alpha_i, \beta_i, i = 1, 2, ..g)$ called characteristics that can only take two values, namely $(0, \frac{1}{2})$ (Atiyah,1971,Mumford,1971). The charged nature of the Riemann surface makes the theta function a voltage function. The key requirement for the Riemann theta function to properly describe a Riemann surface is that it must satisfy a non-linear identity called the Fay trisecant identity.

We now proceed to explain why signals generated by local pinch deformations are soliton solutions of the non-linear Schroedinger differential equation. The idea is to use the Fay trisecant identity. Mumford (Mumford,1987) showed that under pinch deformations (Fig 2) the Fay identity becomes a one dimensional non-linear differential equation so that the response of a Riemann surface to local pinch deformations,described in terms of the Riemann theta function, are one dimensional pulses on the Riemann surface defined by theta function solutions of the non linear Schroedinger differential equation. In the pinch limit the Riemann theta function variables become points inside a tube of the Riemann surface that move obeying the non-linear Schroedinger equation. (Arberello,2001, Kalla 2011)

Thus the result follow, as we now show, from a Principle of Compatibility, which states that all allowed Riemann surface local deformations of our surface network should preserve its mathematical structure as a Riemann surface. Thus local deformations introduced that deform the coordinate variables of the surface and can even change the nature the Riemann surface, should do so by following a path where at every step there is a Riemann surface structure present. At each step of the deformation the local topological coordinate variables of the Riemann surface change. This in turn deforms the variables of the associated Riemann theta function. Input deformations that generate soliton solutions are local pinch deformations. They reduce the circumference of tubes of the Riemann surface to zero as shown in Fig 2. In this limit the Fay non-linear identity becomes a one dimensional non-linear Schroedinger differential equation (Arberello,2001). Compatibility of the Riemann theta function with this deformed Riemann surface structure thus requires that it must be a solution of this non-linear differential equation. Hence solutions of non linear Schroedinger equations represent the response of the surface to pinch deformations.

The emergence of the non-linear Schroedinger differential equation requires that the Riemann surface chosen belongs to a special class (Arberello, 2001), which has a modular structure which means that it has multiple subunit that can act as independent subunits for signal generation. The one dimensional action potential-like soliton voltage pulses generated by a subunit carry charge. As these charged pulses move through the network they generate a transient helical magnetic field that acts on the surface magnetic spin half particles assumed to be present and align them to form a non transient helical structure, held in place by the spin-spin magnetic interactions. The structure is topologically stable. The structure produced reflects the nature of the transient magnetic field that created it which in turn reflects the nature of the moving action potential like signal that carries information regarding the pinch deformation input signals. The structure is thus a memory substrate. It has a natural excitation frequency that can be theoretically estimated to be in the range $(1-30+)$Hz. Suggesting that this frequency label of a memory maybe utilized to recall a memory by a resonance excitation process. The mathematical details are in Sen(Sen, 2021).

Now establish the main result of the paper, namely that whenever a soliton excitation or any other non linear excitation is generated linear surface waveforms that are EEG like waveforms are co-produced. With this step we have a mathematical scheme for generating all observed brain electrical excitations. The key step is the observation that pinch deformations of a subunit reduce its genus to zero, that is, whenever a one dimensional soliton pulse is generated a spherical surface is created as shown in Fig 2 and that on this spherical surface there are input soliton signals. Thus if we consider the spherical surface to be a neuron surface then input soliton signals enter its soma via dendrites are the relevant input signals that lead to soliton production.

The spherical surface created, a neuron surface, is expected to be in an excited electrical state and have surface voltage oscillations. Our aim is to determine the properties of these oscillating waveforms. They are identified as EEG waveforms.

## Results

First we show that the nature of the surface waveform on a spherical surface is determined by the topological charges carried by soliton excitations. To do this we need to identify the waveforms of the wave equation on the surface of a sphere, define the topological charge carried by a soliton and show how this charge determines the nature of the surface waveform.

## Creating Surface waveforms

A general wave equation has the structure,

$$\frac{1}{c^2}\frac{\partial^2\phi}{\partial t^2} - \nabla^2\phi = 0$$

where $\nabla^2$ is the Laplacian operator. For oscillations on the surface of a sphere the Laplacian should have the symmetry of the sphere. This leads to the wave equation becoming a linear second order hypergeometric differential equation (Miller 2010) with three regular singular points (Yoshida,1987). We are interested in waveform solutions that fit together on a spherical surface to cover its surface without overlapping as these special waveforms will persist and should have observable special features. These waveforms thus provide a symmetric tiling of the surface of the sphere. Thus the topological method of generating action potential like soliton signals remarkably suggest that waveforms that tile the sphere should be co-produced and should be observed. These are the observed EEG waveforms that belong to special frequency bands.

Properties of waveform that are solutions of the hypergeometric differential equation with three regular singular points are discussed in Appendix A where it is shown that they are determined by certain phases associated with the three regular singular points of the equation(Yoshida,1987). These phases form a mathematical group, called the monodromy group and if the group is finite the waveforms, tile the sphere surface.

For our problem we identify the three regular singular point locations as three input points for the topological charges carried by solitons enter the cell body and explain how the topological charges, to be defined shortly, fix the monodromy group and thus determine the nature of waveforms created. Furthermore the monodromy groups generated by soliton topological charge inputs can be shown to have finite order so that the waveforms created tile the sphere.

If there are more than three input solitons to the cell body an appropriate generalized hypergeometric equation with more than three singular points is required and is available. Solutions of this equation are also fixed by phases but the solutions are non tiling and are not uniquely determined by the input topological phases(Yoshida 1987). In this case knowledge of the ordering of the input phases is also required to uniquely determine a solution. Hence even though oscillations generated by more than three input phase signals may be present they do not form persistent patterns and hence will appear as a random background of oscillations. For this reason we do not consider them any further but focus on the case where only three soliton signals topological phases are involved. Since our mathematical results are intended to represent events on the surface of neurons we note that there is biological support for considering three input pinch deformations since the number of primary dendrites on a soma, that represent points on the soma where input soliton signals enter a neurons, is between five and seven with a median value of between three and four(Oga 2016,Dharani 2015).

## Surface waveform creation by Pinch Deformation Signals

Let us now gather together the ideas discussed. First the topological charge $W$ of a soliton pulse is a phase which can be define in terms of the discrete characteristic labels $(\alpha_i, \beta_i, i = 1, 2, ..g)$ of the Riemann theta function (Sen,2021), introduced earlier. Each characteristic, $\alpha_, \beta_i$ can only take one of two values, namely $0, \frac{1}{2}$, and these variables represent the spin structure present on the Riemann surface in its associated Riemann theta function. The definition of $W$ is $e^{iW} = e^{4i\pi \sum_{i=1}^{g} \alpha_y \beta_i}$.

We next step relate the soliton signal phase twists $W_i, i = 1, 2, 3$ at three points to monodromy group phases. We assume that a unit twist associated with a soliton excitation at a pinch deformation point produces a twist of, $e^{it}$ at a regular singular point of the hypergeometric differential equation on $\Sigma_0$, the topological sphere created. Then a topological twist $W$ produces a twist $(e^{it})^W = e^{itW}$. This twist is, as discussed in Appendix A, is related to the difference between the characteristic exponents of solutions of the hypergeometric equation at that point.

Finally a set of characteristics of the Riemann theta function is said to be an even/odd depending on whether $e^{i\pi W} = \pm 1$. For solitons to be produced the Riemann theta function must have odd characteristic (Sen,2021). Thus we require that the singular point twist $e^{itW}$ matches topological twist factor $e^{i\pi W}$ of the soliton, which must be $-1$. Thus we have the matching condition $e^{itW} = -1$. This fixes the allowed values of $t$. Possible values of $t$ are $\frac{\pi}{2}, \frac{\pi}{3}, \frac{\pi}{4}, \frac{\pi}{5}$ corresponding to $W = 2, 3, 4, 5$. The monodromy groups generated in this way are of finite order and are hence, by a mathematical theorem, is a tiling solutions that are related to the five Platonic solids of antiquity.(Yoshida,1987)

## Identifying Special Solutions of the Hypergeometric equation

Explicit tiling soltions of the linear hypergeometric differential equation on a sphere were studied by Schwarz,(Schwarz,1873). We will comment on these solutions before we proceed to write down explicit expressions for EEG waveforms and find a formula for the waveform's oscillation frequency for a subclass of Schwarz solutions with the important property that they form a complete set of basis functions on a spherical surface. Thus all possible sphere oscillations can be written down in terms of them.

## Schwarz List of solutions

Schwarz (Schwarz,1873) found 15 algebraic solutions tiling solutions of the second order linear hypergeometric differential equation on the surface of a sphere. Let us give an intuitive reason for this remarkable result. Three facts are helpful.

The first is a property of spherical triangles drawn on the surface of a sphere of radius $R$ with sides that are great circles. Euclid's result that the sum of the angles $\alpha, \beta, \gamma$ of a triangle on a plane add up to $\pi$ radians is now replaced by the result that the sum of angles of a spherical triangle is related to its area in the following way (Wolfram):

$$\alpha + \beta + \gamma - \pi = \frac{A}{R^2}$$

where $A$ is the area of the spherical triangle. Thus the sum of the angles fixes the area of a spherical triangle for a given radius $R$. Hence given that a sphere of radius $R$ has area $4\pi R^2$ we can find the allowed identical set of triangle that can tile the sphere. This leads to five cases discovered by Plato: the five Platonic solids whose surfaces suitable mapped on to the surface of a sphere tile it using identical subunits.

The second fact, stated before, is that the Laplacian operator necessary to study waves on must have the symmetry of a sphere. This requirement leads to the second order hypergeometric differential equation (Miller 2010).

The third fact, also stated earlier, is that the second order hypergeometric differential equation has two linearly independent solutions with three regular singular points and that these two independent solutions are completely determined by the way they change as they are transported round singular points (Yoshida,1987)(Appendix A). Such a transport produces a phase change of the solution called its monodromy, which is a phase angle. The presence of three regular singular points leads to three angles. These angles, if they have the right set of values, can be represented as the angles of a spherical triangle and that can tile the sphere. This means that these waveforms cover the surface of the sphere without overlapping and thus persist stably. For this to happen the solutions have to have special values for their monodromy phases. The sides of the triangles are the nodes of the waveforms. A mathematical description of the way tiling of spheres and special solutions of the hypergeometric differential equation are related is outlined in Appendix A.

A list of such solutions is available (Vidunas 2008,2009). Examples of tilings are shown in fig 4: Schwarz Triangles

## Surface waveform Frequency Estimates

We can give a simple geometric argument to estimate the frequencies of tiling solutions.

The wave like nature of tiling solutions comes from from the fact that they have a periodicity that is induced by the tiling. A solution in one tiling sector has to smoothly join onto the solution in the next sector. This periodicity generates a two dimensional waveform. The size of these two dimensional excitations can be estimated by the area of a tiling segment. If we take the speed of these waves to be approximately tiling independent then we can estimate

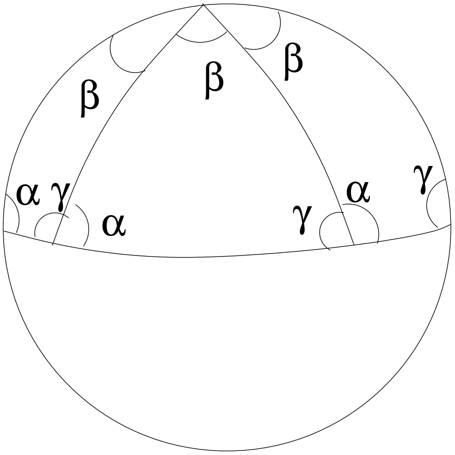

**Fig. 4** Schwarz Tiling.

the frequency of the different waves as being proportional to the inverse of their size.

Let us carry out this frequency estimate for 5 algebraic solutions of Schwarz and then compare our frequency estimates with observed EEG frequencies. The favorable agreement is noted but we continue to treat these results as mathematical results of our surface network The tilings are described by three angle labels $a, b, c$ that fix the tiling area $A$, for a spherical triangle, is fixed by by angles of the triangle by the simple formula $\frac{A}{r^2} = a+b+c-\pi$, where $r$ is the radius of the sphere. We tabulate the tiling areas, estimated wave frequencies and state the associated Platonic solid:

| **Solid** | **Area** | **Schwarz labels** |
|---|---|---|
| Dihedral | $\frac{p}{n}$ | $(\frac{1}{2}, \frac{1}{2}, \frac{p}{n} \leq \frac{1}{2})$ |
| Tetra | $\frac{1}{6}$ | $(\frac{1}{2}, \frac{1}{3}, \frac{1}{3})$ |
| Tetra | $\frac{1}{3}$ | $(\frac{2}{3}, \frac{1}{3}, \frac{1}{3})$ |
| Cube | $\frac{1}{12}$ | $(\frac{1}{2}, \frac{1}{3}, \frac{1}{4})$ |
| Icosa | $\frac{1}{30}$ | $(\frac{1}{2}, \frac{1}{3}, \frac{1}{5})$ |
| Icosa | $\frac{1}{15}$ | $(\frac{2}{3}, \frac{1}{5}, \frac{1}{5})$ |

The areas are in units of $\pi$. The Schwarz labels are the angles $a, b, c$ written as $a = \frac{\pi}{p}, b = \frac{\pi}{q}, c = \frac{\pi}{s}$. The frequencies are proportional to the inverse of the areas listed. We set the basic frequency equal to one Hertz. We then have the frequency estimates,

| **Solid** | **Size** | **Frequency** | **EEG** | **Predicted** | **Observed** |
|---|---|---|---|---|---|
| Dihedral | $\frac{p}{n}$ | $\geq 2$ | All waves | $\frac{1}{n}A$ | All waves |
| Tetra | $\frac{1}{3}$ | 3 | delta (.5-3) | $200\mu V$ | $200\mu V$ |
| Tetra | $\frac{1}{6}$ | 6 | theta(3-8) | $100\mu V$ | $50\mu V$ |
| Cube | $\frac{1}{12}$ | 12 | alpha(8-12) | $50\mu V$ | $50\mu V$ |
| Dodaca | $\frac{1}{15}$ | 15 | beta(12-30) | $40\mu V$ | $< 50\mu V$ |
| Icosa | $\frac{1}{30}$ | 30 | gamma(30–42) | $20\mu V$ | $10\mu V$ |

We compare our mathematical results with the observed 5 types of global EEG brain wave frequencies, namely, the delta (.5-3 Hz), theta (3-8 Hz), alpha (8-12 Hz), beta (12-30 Hz), and gamma (30-42 Hz) are listed ( Liu ,2013). The predicted frequency values setting the base frequency to one hertz are listed. Thus our estimates roughly agree with observations. This encouraging result is a first step in our identifying the surface network signals as brain signals and the surface oscillations that we are studying as EEG waveforms. For the moment we continue to carry out our mathematical analysis and regard the comparison result as an interesting coincidence. To get the frequencies a base frequency of one Hertz was chosen and the sphere radius $r$ was set to one. For arbitrary $r$ the frequencies scale by the factor $\frac{1}{r^2}, r > 0$. However we have set the basic frequency to be one hertz. This fixes the scale. Thus setting $r = 1$ is justified. It is not an extra parameter of the model. The amplitudes numbers predicted use an input value of $200\mu V$ for delta waves.

We also note that since the Schwarz solutions are solutions of a linear system, a general surface waveform will be a linear superposition of the fundamental set of eigensolutions of the system.

## Surface Waveforms: Fractional Legendre functions

We now determine analytic expressions for waveforms and find an explicit formula for their allowed frequencies of tiling solutions for a sub class of tiling solutions that give dihedral, tetrahedral, and cubic tilings. This sub class waveforms can be represented by associated Legendre functions of fractional order, $P_\nu^\mu(z)$. For this class we can write down explicit analytic expressions for the waveforms and find an explicit formula for their oscillation frequencies: the solutions also form a complete set of basis functions (Maier, 2018) so that they can be used to represent any arbitrary square integrable function $f(z)$ on the sphere. Thus, any such function $f(z)$, can be written as,

$$f(z) = \sum_{n=-\infty}^{i=+\infty} c_n P^{\mu}_{\nu_0+2n}(z)$$

where the points $z$ represent arcs on the sphere. From this result and the orthogonality property,

$$\int_{z=-1}^{z=+1} P^{\mu}_{\nu_1}(z) P^{-\mu}_{\nu_2}(-z) = \alpha(\mu, \nu_1)\delta_{\nu_1,\nu_2}$$

we obtain the completeness result,

$$\delta(z - z') = \sum_{n=-\infty}^{n=+\infty} \frac{P^{\mu}_{\nu+2n}(z) P^{-\mu}_{\nu+2n}(-z')}{\alpha(\mu, \nu + 2n)}$$

The dihedral tiling class corresponds to setting $\mu = \frac{1}{2}, \nu = -\frac{1}{2}$. We also have the completeness result,

$$\delta(t-t') = \int d\omega e^{i\omega(t-t')}$$

A more general class of basis functions can also be used for representing functions defined on the sphere rather than along arcs on the sphere. They are the analog of the usual spherical harmonics. We display the ones related to dihedral tiling. We have

$$Y^{-\frac{1}{2}}_{-\frac{1}{2}+2n}(\theta,\phi) = N_{(\frac{1}{2},2n-\frac{1}{2})} e^{-i\frac{\phi}{2}} \sqrt{\frac{8}{\pi \sin\theta}}\ \cos(2n - \frac{1}{2})\theta)$$

where $n = 1, 2, ..$ and $N_{(-\frac{1}{2},2n-\frac{1}{2})}$ is a normalization factor. It is evaluated in the next section. Using this function we can plot EEG waveform-s in two dimensions and display their tiling property.

The completeness property of these solutions and the fact that they are related to solutions of the wave equation on a sphere will now be used to construct a Greens function(Morse, 1953) appropriate for studying space-time dependent modulations of the surface waveforms.

## Construction of Greens function for surface wave modulations

The Greens function $G(z, t : z', t')$ satisfies the equation,

$$(\frac{1}{c^2}\frac{\partial^2}{\partial t^2} - \nabla^2)G(z, t : z', t') = \delta(t-t')\delta(z-z')$$

We next replace the right hand side with the delta function representations chosen, with $\mu = \frac{1}{2}, \nu = -\frac{1}{2}$, and use the complete set of dihedral tiling waveforms to write,

$$G(z, z', t-t') = \sum_n \int d\omega \frac{P^{\mu}_{\nu+2n}(z) P^{-\mu}_{\nu+2n}(-z')}{(-(\frac{\omega^2}{c^2}) + \omega^2_n)} \frac{e^{-i(t-t')\omega}}{\alpha(\mu, \nu+2n)}$$

where $\nabla^2 P^{\mu}_{\nu+2n}(z) = -\omega^2_n P^{\mu}_{\nu+2n}(z)$ and we have assumed that the Greens function depends only on $(t-t')$. Carrying out the $\omega$ integral we get

$$G(z, z', t-t') = i\pi \sum_n (\frac{e^{-i\omega_n(t-t')}}{\omega_n}) \frac{P^{\mu}_{\nu+2n}(z) P^{-\mu}_{\nu+2n}(-z')}{\alpha(\mu, \nu+2n)}$$

The modulation $m(z, t)$ of an surface waveform due to an input signal $s(t, z)$ can now be calculated. We have

$$m(z, t) = \int dt' \int dz' G(z, t, z', t') s(z', t')$$

The dihedral tiling waveforms, labeled by an index $n$, have frequencies

$$\omega_n = \sqrt{n^2 - \frac{1}{4}}, \quad n = 2, ..$$

and their waveform shapes are given by the fractional spherical harmonics,

$$Y_{n-\frac{1}{2}}^{-\frac{1}{2}}(\theta, \phi) = N_{(-\frac{1}{2}, n-\frac{1}{2})} \; e^{-i\frac{\phi}{2}} \sqrt{\frac{8}{\pi \sin\theta}} \; \cos(n - \frac{1}{2})\theta$$

where $n = 1, 2, ..$ . Thus we have found explicit expressions for surface waveforms and a formula for their allowed frequencies.

We can next relate the frequencies of these waveforms to their amplitude by calculating the normalization factor $N_{(-\frac{1}{2}, 2n-\frac{1}{2})}$. This will determine the way it scales with $n$ and thus establish a relationship between the amplitude and the frequency of a waveform. Using the normalizations of Maier(Maier 2018) for $P_\nu^\mu(\theta), P_\nu^{-\mu}(\theta)$ that can be related their norm $P = P^2 = \int_\pi^{+\pi} d\theta \sin\theta P_\nu^\mu(\theta) P_\nu^{-\mu}(\theta)$ can be evaluated. Writing $P_\nu^\mu(\theta) \to P\frac{P_\nu^\mu(\theta)}{P}$, with $(\mu = \frac{1}{2}, \nu = 2n - \frac{1}{2})$ the $n$ dependence of the amplitude is fixed by $P$ which is,

$$P \; = \sqrt{\sqrt{\frac{2}{\pi}} \; \frac{\Gamma(\frac{3}{4})}{\Gamma(\frac{5}{4})} \; \frac{(4n+2)}{(2n+\frac{1}{2})(2n+\frac{3}{4})}}$$

Thus a clear inverse relationship between the amplitudes and frequencies is established. Since the dihedral tilings can be used to represent all other tiling solutions, this relationship is valid for all surface waveforms.

There are corresponding set of basis functions for some other tiling waveforms. For, example, for a tetrahedral or octahedral tiling generated surface waveforms, the frequencies are of the form,

$$\omega = \sqrt{(\nu + \frac{1}{2} + 2n)(\nu + \frac{3}{2} + 2n)}$$

with appropriate fixed values for $(\nu, \mu)$ and $(n, m)$ integers $(0, 1, 2, ..)$ that reflect the symmetry of the tiling, there is a corresponding waveform $Y_{\nu+\frac{1}{2}+2n}^{\mu+m}(\theta, \phi)$. These expressions may be directly used also show the inverse relationship between waveform amplitudes and their frequencies. Thus, for the octahedral tiling case an explicit expression for waveforms is available (Maier 2018). We have,

$$P_{-\frac{1}{6}+n}^{\frac{1}{4}+m}(\cos\theta) \; = \; 2^{-2m-3n} \; \Gamma(\frac{3}{4} - m)^{-1} \; (\sin\theta)^{-\frac{1}{4}-m} B_+^{\frac{1}{4}+3m+3n} r_n^m(\frac{B_-}{B_+})$$

$$B_\pm \; = \; \cos(\frac{\theta}{3}) \pm \sqrt{\frac{4\cos^2(\frac{\theta}{3}) - 1}{3}}$$

where $r_n^m(\frac{B_-}{B_+})$, for $(n,m) \geq 0$ are Heun polynomials (Ronveaux 1995) of degree $(3n+2m)$ with octahedral symmetry. However we will not consider these cases any further and in all our subsequent work and discussions we will always use the dihedral waveforms to approximate all other tiling solutions and thus represent all surface waveforms.

At this stage we have the mathematical tools required to study the response of the surface waveforms to signals and we have found the waveform oscillation frequencies and their explicit form. We now take the next step and assume that the soliton excitations of our network represent brain signals and our surface oscillations co-produced with any signal created by pinch deformations as EEG waveforms. We thus identify multi-soliton solutions with spike trains, dark soliton solutions that are oscillations on top of a high energy background, with bursts and transient localized excitations that can be generated by pinch deformations, with blocking signals that prevent certain certain brain circuits from functioning, as observed during sleep (Sen,2021). We can then apply the techniques established to analyze observed EEG events.

We carry out such an analysis to discuss the observed sequence of brain EEG events during deep sleep (NREM),namely, K-complexes-Sleep-Spindles and Sharp -Wave Ripples.

## Modeling K-complexes-Sleep-Spindles-Sharp Wave Ripples

In NREM sleep delta waves are observed and at intervals of 1-1.7 minutes large sharp spikes, K-complexes, are seen that have amplitudes in excess of 100 mV in the background high amplitude of slow waves and delta waves (1.6-4.0) Hz present. These excitations have duration in excess of 500 ms and are followed by spindle shape oscillations of duration a few seconds of frequency in the range $(10-15)$ Hz, followed by sharp wave ripples (De Gannaro 2003,Ioannides 2019). The events described happen in this order.

We now show that we can interpret this sequence of events as a mechanism of memory consolidation and the transference of memory copies from one region of the brain, possibly the hippocampus, to another region of the brain, possibly the frontal cortex (Buzsaki 1989, 2015) in the framework of our topological surface network . The first step in the sequence of events described is thus assumed to be due to a major transient localized cortical that prevents regions of the brain from receiving or processing information for the period of time. It is a local blocking event. The triggering event should have high voltage, be transient, and localized to an appropriate brain region with a duration in excess of 500 ms. During this period of time other signals cannot proceed in the region where the event has occurred: the region is thus isolated from other signals. Such a blocking transient event, we suggest is responsible for the K-complex modulation of the delta wave that is co-produced with it. A mathematical example of such a transient cortical event which can be created by pinch deformation input signals, exists. Examples are rational breather and peakon solutions(Kalla 2011).

We next suggest that sleep spindles observed reflect the modulation of delta waveforms by the natural frequency excitation of a helical magnetic memory structure (Sen et al 2021, submitted). It was shown that the structure has a natural excitation frequency in the range $(1 - 30+)$ Hz (Sen 2021).

Finally the memory trace modulation on the high voltage delta waves interact with underlying neurons to produce, by a resonance process, a memory copy carrying burst excitations which, in turn, modulate the delta waveforms co-produced and shows up as sharp wave ripples in the EEG signals. The produced bursts are interpreted as copying and transferring memory information. Because of the extensive nature of the blocking signal the visual and auditory sensory pathways do not respond to these activities.

In earlier work (Sen et al. 2021) it was shown that memories may be stored non-locally as closed helical magnetic traces $\Delta\vec{B}(x)$ in the pathways traversed by multi-soliton excitations. The non transient trace has a natural excitation frequency in the oscillation frequency range $(1 - 30+)$ Hz. We now calculate the modulation of a delta waveform potential as it moves over such a magnetic memory trace. In an earlier section we showed that the delta waveform potential was $V(\theta, \phi, t) = Ne^{-i\frac{\phi}{2}}\sqrt{\frac{8}{\pi \sin\theta}}\ \cos(2n - \frac{1}{2})\theta\ e^{i\omega_0 t}$,in terms of spherical polar coordinates, with $\frac{pi}{2} < \theta < \pi$, where $N$ was a normalization constant and $\omega_0 = \sqrt{n^2 - \frac{1}{4}}, n = 2$. Using this expression we can calculate its the gradient $-\nabla V$ which is an electric field that acts on charges $e$ on the tube causing them to move. For a qualitative understanding of this effect, which we show these effects produces spindles, we replace the $(\theta, \phi)$ dependence of $V(\theta, \phi, t)$ by a simpler expression but we retain its theoretically motivated time dependence. Thus we set $V = V_0 \sin\theta \sin\phi \cos t$ for the delta waveform, so that $\omega_1 \approx n$. Then $V = V_0 y \cos t$ in Cartesian coordinates and we have,

$$\begin{aligned} E_y &= -\nabla_y V = V_0 \cos t \\ m\frac{dv_y}{dt} &= eE_y \\ v_y(t) &= \frac{V_0 e}{m}\sin t \end{aligned}$$

This moving charge interacts with the helical magnetic trace present and excites it to its natural frequency $\omega_0 = \frac{2\pi v_0^2}{cr_s}$ found in Sen(Sen,2021), where $v_0$ is the charged soliton pulse speed that led to the magnetic memory trace. Thus we have the excited magnetic field given by,

$$\vec{B}(t, \vec{x}, r_s) = B(\vec{x})(\cos(\frac{2\pi v_0^2 t}{cr_s}), r_s \sin(\frac{2\pi v_0^2 t}{r_s}), z = v_0 t),$$

where $r_s$ is the radius of the tube, $c$ the velocity of light in the medium.Thus the natural excitation frequency of the structure is $\omega_0 = \frac{2\pi v_0^2}{cr_s s}$. To calculate the modulation of the EEG wave we use the fact that the moving charge interacts with this magnetic field via the electromagnetic Lorentz force (Jackson,1962). Thus if the charge is moving with velocity $v_y$ it interacts with the $x$ component of the magnetic trace, it produces a force in the $z$ direction and hence generates a force $F_z$ from which modulating potential $\Delta V$ can be determined by noting that $F_z dz = -\Delta V$. The force is given by

$$F_z = \frac{e}{c} B v_y(t) \cos \omega_0 t$$

and the modulating potential is $\Delta V = -F_z dz$. Thus we find that $\Delta V$ is,

$$\Delta V = \frac{e^2 V_0}{mc} B(\sin z) \sin(\omega_0 z) dz, \;\; 0 \leq z \leq L$$

where we have used $z$ to parametrize time, setting $B_z = z = v_0 t$ for the helical magnetic memory trace, and we have set $v_0 = 1$. This is a spindle (Fig 5). It carries the helical magnetic memory trace excitation frequency.

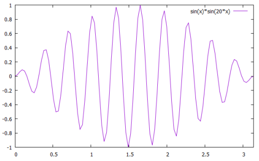

**Fig. 5** Sleep Spindle

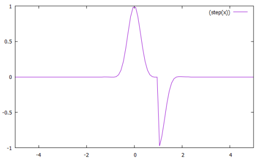

**Fig. 6** K Complex

Thus $\Delta V$, provides a copy of the memory traces. We now interpret our results in terms of brain excitations. The modulation theoretically determined has the shape of a sleep spindle, as $\omega_0 >> 1$. From observations we find that $\omega_0 \approx 10 - 15$ Hz which is consistent with our earlier theoretical result (Sen,2021) that memories are stored non-locally as topologically stable helical magnetic traces with a theoretically determined frequency in the range $(1 - 30+)$ Hz. The result obtained will remain valid even if we had used our theoretically determined expression for the delta waveform potential rather than our simple representation of it. The difference would be in, not in the qualitative shape of the sleep spindle but in its detailed nature as there would now be a spatial dependence present in $\vec{v}(t)$ with the combination $(v_y B_x - v_x B_y)$ rather than just the term $v_y B_x$ that we used.

## Transient Signals and K-complex

We now give the mathematical details that show how the suggestion that a high energy blocking signal, which is a transient solutions of the non-linear Schroedinger equation can explain a K-complex modulation. Explicit mathematical examples of such transient solutions exist, such as the peakon solution and rational breather solution and their analytic forms are available (Kalla 2011) but, we simplify our analysis by approximating the known analytic solutions for transient excitations, using the following simple expression,

$$\psi(\theta,\phi,t) = \delta(\theta-\theta_0)\delta(\phi-\phi_0)e^{-(\omega_n t)^2}\Theta(t) - \Theta(t-\frac{1}{\alpha})\delta(\theta-\theta_1)\delta(\phi-\phi_1)$$

where $(\theta_1 = \theta_0+\Delta, \phi_1 = \phi_0+\Delta)$, and $\Theta(t) = 1, t > 0$ and is zero otherwise, the Heaviside Theta function. The Greens function, for surface dihedral waveforms is given by,

$$\begin{aligned} G(z,z',t-t') &= i\pi(\frac{e^{-i\omega_n(t-t')}}{\omega_n})\ P^{\frac{1}{2}}_{-\frac{1}{2}+2n}(z)P^{-\frac{1}{2}}_{-\frac{1}{2}+2n}(-z') \\ P^{-\frac{1}{2}}_{2n-\frac{1}{2}}(\theta) &= \sqrt{\frac{8}{\pi\sin\theta}}\ \cos(2n-\frac{1}{2})\theta), \end{aligned}$$

For our qualitative discussion we drop normalization factors and ignore the spatial oscillations of the waveforms. Then any surface waveform modulation due to a transient localized excitation, can be plotted (Fig 6) using,

$$\begin{aligned} M(t) &= M_1 + M_2 \\ M_1 &= A\frac{1}{\sqrt{n}}e^{-(\omega_n t)^2}\cos\omega_n t, \quad -T < t < +T \\ M_2 &= A\frac{1}{\sqrt{n}} - e^{-(\omega_n(t-2T))^2}\cos\omega_n t, \quad +T < t < +3T \end{aligned}$$

with $\omega_n = \sqrt{4n^2-\frac{1}{4}}$. For numerical work an appropriate gluing function $M_{12}$ is required. The value of the constant $A$, has to be chosen.

Thus a K-complex modulation of a EEG delta waveform can be understood as a modulation of the delta waveform by a high energy transient blocking excitation. The transient event is required to have high energy, as the delta waveform co-produced with it and then modulated by it, has high energy. But such transient excitations can theoretically exist with lower energies, ranges and duration. We sketch the possible energies, ranges and durations, that such excitations can have, using brain EEG waveform information. We then suggest that all of these transient excitations should be observed and that they all play a role in the functioning of the brain.

## Prediction of Range, Energy and Duration of Blocking Signals

We can predict the duration, range and energies of any one of these theoretically allowed transient excitation that produces K-complex like EEG modulation by linking these parameters to the EEG waveforms that they modulate. Our estimate for duration is, thus, $\tau_n \approx \frac{1}{\omega_n}$, for energy $\approx V$, the voltage amplitude of the waveform, with a range given by the area fraction of a sphere tiled by the waveform. Hence for a delta wave these estimates suggest a duration $\tau_1 \approx \frac{1}{2}$ seconds which is $\approx$ 500 ms (Weigenand 2014). We tabulate the results, listing the $n$ value of an EEG waveform, and the amplitude, in mV, and duration,in ms, of K-complexes EEG modulations created by transient localized excitations.

| **Waveform** | **Wave Number** | **Amplitude** | **Duration** | **Range** |
|---|---|---|---|---|
| Delta | 1 | 100 | 500 | $\frac{\pi}{2}$ |
| Theta | 3 | 30 | 100 | $\frac{\pi}{3}$ |
| Alpha | 6 | 16 | 50 | $\frac{\pi}{6}$ |
| Beta | 10 | 10 | 30 | $\frac{\pi}{10}$ |
| Gamma | 50 | 2 | 6 | $\frac{\pi}{50}$ |

We speculated earlier that a person can perhaps initiate transient localized blocking events by chemical means. Perhaps the local release of dopamine and nitric oxide signals (Kali 2010) play such a role in the case of K-complexes. This is because dopamine has been identified as a system manager for cortical activity (Hong 2013) while nitric oxide has been identified as playing a key role in sleep (Kalinchuk 2010). If this is true then blocking dopamine and nitric oxide signals would stop K-complexes and thus prevent the method of memory consolidation and transfer suggested.

Another implication of this speculation is that those that have a greatly reduced number of K-complexes during NREM should not be able to store long term memories. This speculation can be tested.

## Plotting EEG waveforms in the dihedral approximation

A few representative plot for a waveforms are plotted. These plots clearly show the tiling nature of the waveforms.

We next tabulate the predicted frequencies and amplitudes of a sample EEG waveforms and compared them with observations.

Our first step is to show that the solutions constructed are indeed tiling solutions, which means that they must vanish on the sides of an appropriate spherical triangle on the surface of a sphere. We select the following set,

$$Y^{-\frac{1}{2}}_{2n-\frac{1}{2}}(\theta,\phi) = N_{(-\frac{1}{2},2n-\frac{1}{2})}\ e^{-i\frac{\phi}{2}}\sqrt{\frac{8}{\pi \sin\theta}}\ \cos(2n-\frac{1}{2})\theta$$

where $n = 1, 2, ..$ . The angles $(\theta, \phi)$ are spherical polar coordinate angles with ranges $(0 \leq \theta \leq \pi, -\pi \leq \phi \leq +\pi)$. To construct tiling solutions that vanish on the sides of a spherical triangle the following variable changes are required$\theta \to \theta' = \frac{\theta}{2}, \phi \to \phi' = \frac{\phi}{2n}$ and we require that the solution be periodic

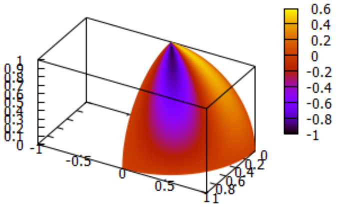

**Fig. 7** EEG Delta Wave

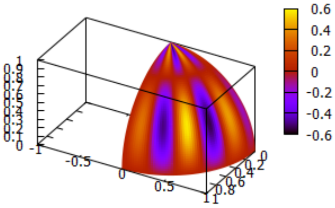

**Fig. 8** EEG Theta Wave

in $\phi'$. In terms of these variables, the solution becomes,

$$S^{-\frac{1}{2}}_{2n-\frac{1}{2}}(\theta', \phi') = \frac{1}{\sqrt{n}} \cos(n\phi') \sqrt{\frac{1}{\sin 2\theta'}} \cos(2n - \frac{1}{2})2\theta'$$

where the range of the angles are now $(0 \leq \theta' \leq \frac{\pi}{2}, -\frac{\pi}{2n} \leq \phi \leq +frac\pi 2n)$. We check that this solution vanishes when $\theta' = \frac{\pi}{2}$ and when $\phi' = \pm\frac{\pi}{2n}$ which define the three sides of a spherical triangle. Thus we have constructed a tiling solution. To plot this waveform the expression obtained should be multipliede by $\sin(2\theta')$. We have included a normalization factor $\frac{1}{\sqrt{n}}$ which is an approximation of $P$ defined by $P^2 = \int_{\pi}^{+\pi} d\theta \sin\theta P^{\mu}_{\nu}(\theta) P^{-\mu}_{\nu}(\theta)$ with $(\mu = \frac{1}{2}, \nu = 2n - \frac{1}{2})$

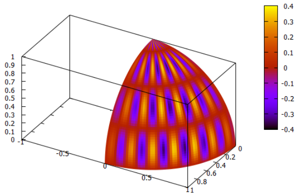

**Fig. 9** EEG Beta Wave

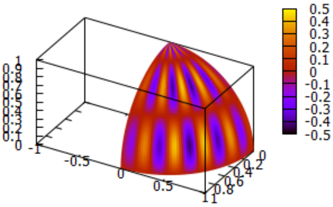

**Fig. 10** EEG Alpha Wave

the $n$ dependence of the amplitude is fixed by $P$[27] which is,

$$P = \sqrt{\sqrt{\frac{2}{\pi}}\ \frac{\Gamma(\frac{3}{4})}{\Gamma(\frac{5}{4})}\ \frac{(4n+2)}{(2n+\frac{1}{2})(2n+\frac{3}{4})}} \approx \frac{1}{\sqrt{n}}$$

It is now clear that the amplitudes are inversely related to frequencies and we list, in tabular form, the frequency and amplitude predictions made for EEG waveforms in this approximation .

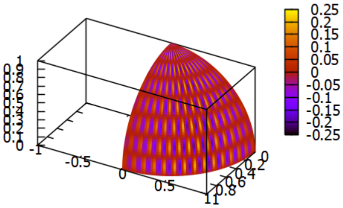

**Fig. 11** EEG Gamma Wave

| **Solid** | **Size** | **Frequency** | **EEG** | **Predicted** | **Observed** |
|---|---|---|---|---|---|
| Dihedral | $\frac{p}{n}$ | $\geq 2$ | All waves | $\frac{1}{\sqrt{n}}A$ | All waves |
| Dihed | $\frac{2}{2}$ | 1 | delta (.5-3) | $200\mu V$ | $200\mu V$ |
| Tetra | $\frac{1}{6}$ | 6 | theta(3-8) | $80\mu V$ | $50\mu V$ |
| Cube | $\frac{1}{12}$ | 12 | alpha(8-12) | $57\mu V$ | $50\mu V$ |
| Dodaca | $\frac{1}{15}$ | 15 | beta(12-30) | $40\mu V$ | $< 50\mu V$ |
| Icosa | $\frac{1}{30}$ | 30 | gamma(30–42) | $28\mu V$ | $10\mu V$ |

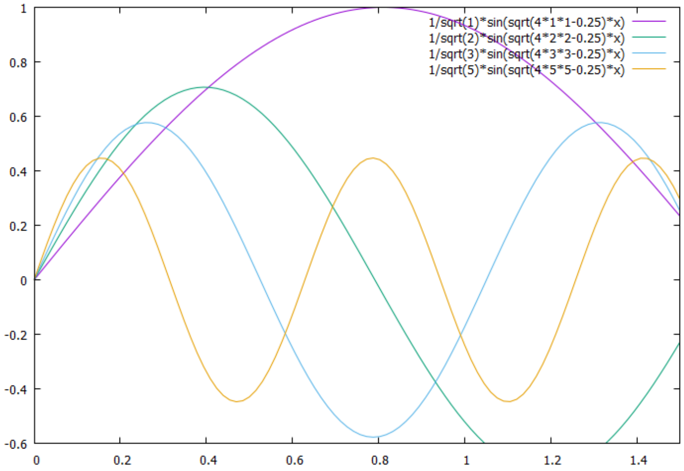

**Fig. 12** Frequency-Amplitude Plots

## Discussion

The central idea of this paper is to show that it is possible to generate all observed brain excitations by exploiting the topological features of the brain's connectivity architecture. This is demonstrated by constructing a surface network that, we proved, exactly captured the topological connectivity of a hypothetical brain connectome and then showing that indeed, if the surface chosen is charged and has a spin structure, it can generate both one dimensional action potential like soliton excitations and co-produce EEG waveform like surface oscillations in response to local input surface pinch deformation signals, by exploiting the topology of the network.

In an earlier paper the first part of signal generation, namely generating action potential-like solitons, was discussed. It was shown that a wide variety of one dimensional soliton pulse signals, whose explicit analytic forms were theoretically determined, could be generated in this way(Sen,2021). The surprise was that these soliton signals carry with them topological information about the network as well as information about the input pinch deformation signals that create them and can transfer this information to the pathways they traverse leaving a surface helical spin aligned non transient magnetic memory trace. The memory trace is a magnetic alignment of surface spins that is topologically stable and has a natural, theoretically estimated, excitation frequency. Thus memory storage, in the scheme, is a non local magnetic trace in the pathways between engram cells(Queenan,2017).

Here we showed how the topological surface network also co-produce EEG waveform like surface oscillations whenever non linear one dimensional action potential like solitons or any other non linear excitation, generated by local pinch deformations is generated. The explicit form and frequency bands of these EEG waveforms co-produced, were theoretically determined and a precise relationship between a soliton excitation's topological charge and the nature of the EEG waveform it co-produces was found. It was shown that the oscillation frequencies must belong to five discrete classes that correspond to the Platonic tiling of a spherical surface, and that there is an inverse correlation between the frequency of a waveform and its amplitude. These theoretical predictions were found to be consistent with observations. A further general prediction was that EEG waveforms have a universal nature, that is, they should have the same structural properties for all creatures that have a mammal like neuron-synapse architecture(Bullough,2002, Fingelkurts 2014).

The method of EEG waveform generation proposed here is unconventional. (Nunez 2006a,2006b, DaSilva, 1991, 2010,Jones,2016,Klimeschi,2018). It differs from other approaches in several ways: it treats all EEG waveform generation as excitations co-produced with action potential in a uniform way that predicts how the nature of the EEG waveforms are determined by the action potential. It directly predicts the universal nature of EEG waveforms and establishes that the EEG waveform frequencies are inversely related to their amplitudes and that EEG waveform frequencies although predicted by action potentials, as shown, are fixed by geometry and not related to action potential spike train frequencies.

We speculated that EEG waveforms co-produced play an essential role in the functioning of the brain based on the mathematical results obtained. For instance ,our discussion of the K-complex initiated sequence of EEG events, can be interpreted as a dialog between action potentials soliton pulses or other non-linear effects produced by pinch deformation input signals and the EEG waveforms co-produced by them. The start of the K-complex sequence was assumed to be due to a high energy transient localized pinch generated excitation. This event blocks other signals from accessing certain brain circuits and can be represented as a pinch generated rational breather or peakon solutions of the non linear Schroedinger equation(Kalla,2011). This transient blocking signal co-produces a high energy EEG delta waveform that is then modulated by the transient signal, as we showed, to produce the K-complex shape observed. The sleep spindles that follows was interpreted as the modulation of a delta waveform interacting with the helical excitation frequency of a magnetic memory trace (Sen, 2021). It represents a memory copy in the form of a oscillating voltage profile. This high energy oscillating memory voltage profile then excites neurons it covers to produce a burst (a dark soliton excitation), that shows up as a sharp wave ripple on the delta waveform.The sequence of event can thus interpreted as a method of transferring a memory copy due to the cooperative interaction between nonlinear excitations and EEG waveforms.

The hypothesis that blocking signals can co-produce EEG waveforms is supported by observations(Becker 1985).

Transient localized blocking signals, we speculate, maybe universal. Theoretically they can have a wide range of energy and duration values that depends on the way they are generated by pinch deformations (Kalla,2011). We speculate that they play a role in both REM sleep and indeed in other cognitive functions of the brain, such as focused attention. For REM sleep the transient blocking signals are less energetic and have smaller range and do not block visual and possibly auditory sensory pathways. If this is the case then we suggest that the blocking signals co-produce the less energetic theta waveforms which are now modulated by brain memory trace excitation l frequencies, estimated (Sen,2021) in the frequency range $(10-16)$Hz. The analogue of sleep spindles created, in this case, will look more like beta waves and the interaction between the theta waveforms and stored memory will stimulate and consolidate memories during which we experience dreams. This speculation predicts that dreaming should be a universal experience for all mammals. Just as a high energy blocking excitation shows up as a K-complex followed by sleep spindles on delta waveform modulation in NREM sleep, a less energetic blocking event should be present before the onset of REM. Perhaps they are the sawtooth wave modulation on theta waveforms observed (Suvadi 2015) before the onset of REM.

Let us next speculate on the way such signals could provide a mechanism for focused attention. A low energy transient localized excitation would stop local access of certain signals thus permitting only signals of interest to be processed. At the same time the blocking excitation would co-produce EEG waveforms that would be able to access locally stored memories labeled with frequencies that overlap with those of the EEG waveform generated (Colgin,2009). Such a resonance mechanism could help identifying the nature of the incoming signal and at the same time recall relevant memories required for focused attention. We speculate that a person can produces the low energy transient blocking signals required for this constantly possibly by chemical means.

Summarizing: soliton pulse excitations are generated by local pinch surface deformations, they carry the pinch deformation information and store it non-locally as a magnetic structure that has a natural theoretically estimated excitation frequency, while transient localized blocking signals can have a wide range of energy and duration values. They can also be generated by pinch deformations. It is speculated that these pinch deformations result from selective chemical releases and that both soliton pulses and transient localized excitations co-produced EEG waveforms that work together to carry out the cognitive functions of the brain. We suggest that EEG waveforms are the muscles of thinking.

All our results follow from the topological and smoothness properties of a mathematical surface network that we proved exactly captures the topological connectivity properties of a brain connectome. In view of the predictive nature of the scheme it seems worthwhile to examine it in greater detail. The scheme suggested maybe a useful mathematical representation of the brain.

## Declarations

1. This research did not receive any specific grant from funding agencies in the public, commercial or not-for-profit sector.
2. The authors declare no competing financial interests.
3. Availability of data and methods (not applicable)
4. Code availability (not applicable)

## Appendix A: Monodromy Groups and Tiling angles

The tiling surface waveforms were shown to be special solutions of the linear hypergeoemetric equation and a way to co-produce them by pinch deformation excitations was described. Here we define the monodromy group of the differential equation and explain the link between the monodromy groups and tiling angles required to get the Schwarz solutions.

The hypergeometric equation solutions has two linearly independent solutions and its regular singular points, are chosen to be at $0, 1, \infty$. Each solution has characteristic exponents. Suppose $b_0, b_1, b_\infty$ are the inverses of characteristic exponent differences of the hypergeometric differential equation near the singular points $0, 1, \infty$. We now recall that the hypergeometric equation can be written as,

$$x(1-x)\frac{d^2u}{dx^2} + (c - (a+b+1)\frac{du}{dx} - abu = 0$$

In terms of these parameters we have $\frac{1}{b_0}$ = 1-c, $\frac{1}{b_1}$ = c-a–b, $\frac{1}{b_\infty}$ = a-b, where the terms 1-c, c-a-b, a-b are the characteristic exponent differences of the given hypergeometric equation at its three singular points $x = 0, x = 1, x = \infty$ respectively.

The hypergeometric equation has an underlying group structure. It can be obtained as an eigenvalue equation of the Casimir operator of the Lie algebra $SL(2, C)$ (Miller 2010,Kitaev 2018). The group $SL(2, C)$ represents the symmetry of the sphere. Explicitly the group acts on a a point $z$ of the upper half plane mapping it to a point $w$ by $w = Mz$, where $M$ is a $2 \times 2$ $SL(2, C)$ matrix with complex coefficients $a, b, c, d$ as,

$$\begin{aligned} w &= \frac{az+b}{cz+d} \\ ad - bc &= 1 \end{aligned}$$

The hypergeometric functions also appear as the representaion of the Lie algebra of the group $SL(2, C)$ (Miller 2010) that is the symmetry of the Riemann sphere. The three regular singular points of the hypergeometric equation can be taken to be three points on a sphere. A curved triangle can be drawn on this sphere with these three points as its vertices. The spherical angles between the lines of this curved triangle are chosen to be associated to difference between characteristic exponents of the two linearly independent solutions of the hypergeometric equation at that regular singular point. Thus a solution, described by its characteristics has a geometric representation as a curved triangle on the surface of a sphere.

## Fixing the tiling angles

The reason why differences of exponents appear in the analysis can be understood as follows: by analytic continuation (Yoshida 1987) a pair of linearly independent solutions can be extended to all points inside the triangle, the upper half plane and then, by using a reflection principle, (Yoshida 1987) to the lower half plane and thus extended to the entire sphere provided the characteristic exponents of the solutions are special. Such an extension can represent a tiling of the sphere.

Now consider the set $S = (0, 1, \infty)$ of the regular singular points of the hypergeometric differential equation and define $X = C^2 - S$, where $C^2$ is the two dimensional complex plane and $x_0$ a point in $X$. The hypergeometric differential equation has two linearly independent solutions, say $u_1, u_2$ in the neighborhood of a singular point. If we continue these solutions $u_1, u_2$

analytically along a curve $C$ in $X$ then we get

$$C_*^t(u_1, u_2) = M(C)^t(u_1, u_2)$$

where $M(C)$ is a non singular two-by-two matrix and $C_*$ represents the analytic continuation of $u_1, u_2$ along the curve $C$. The matrices $M(C)$ for different curves forms a representation of the fundamental group of $\Pi(X, x_0)$ and is called the monodromy representation of the differential equation. The monodromy group representation for $\Pi(X, x_0)$ can be constructed from the characteristic exponents of the equations at its singular points. Explicitly if $v_1, v_2$ are the analytic continuations of $u_1, u_2$ we can write,

$$\begin{aligned} v_1 &= au_1 + bu_2 \\ v_2 &= cu_1 + du_2 \\ \frac{v_1}{v_2} &= \frac{au_1 + bu_2}{cu_1 + du_2} \\ &= \frac{a\frac{u_1}{u_2} + b}{c\frac{u_1}{u_2} + d} \\ ad - bc &= 1 \end{aligned}$$

Thus if $u_1 \approx z^\alpha, u_2 \approx z^\beta$ near a regular singular point, where $\alpha, \beta$ are characteristic exponents then the difference of the exponents appear naturally as parameters when we consider ratios of solutions. This is a projective way of studying the solutions. The mondodromy group has the as a linear fractional $PGL(2, c)$ transformation. It is a projective group.The group maps the ratio of appropriate solutions of the hyperheogeometric are real interval in the intervals $(0, 1), (0, \infty), (1, \infty)$. If we consider the strip of the upper half plane with $(0, 1)$ as the real axis then this strip is mapped to the curved triangle joining the point $0, \infty$ and $1, \infty$. The point $\infty$ is the north pole of the sphere. If such triangle has angles, given by the $\pi$(difference between critical exponents) in Schwarz list then by the action of the finite triangle subgroup of $PGL(2, C)$ these triangles tiles the upper half plane. Then by using a reflection principle of Schwarz (Yoshida 1987) this tiling can made to cover the entire sphere provided the spherical triangles have special angle values. Thus special solutions of the hypergeometric equation give a tiling of the sphere. The fact that the group of projective fractional linear transformations $PGL(2, C)$ maps circles and lines to circles and lines and preserves angles is used in the construction described.

The monodromy group $PGL(2, C)$ describes the way twists present at three specified singular points, given by the characteristic exponent differences, fit together. For the hypergeometric differential equation on the sphere this information completely fixes the solutions of the hypergeometric equation(Yoshida 1987).

# References

[1] Arberello,E. Sketches of KdV, Contemporary Mathematics,312,9-70,(2001)

[2] Atiyah,M.,Spin Structures. Ann.Scientifique de l'Ecole Normale Superieure, Quatrieme, Series, 4, 47-62,(1971)

[3] Bievins.A.S.,Bassett.D,Topology in Biology,ISBN:978-3-319-70658-0(2020)

[4] Becker,R. and Seldon,G.The Body Electric, New York, Morrow, pages111-113,(1985)

[5] Bullock, T.H.,How do Brain Waves Work? Papers of a Neurophysiologist, Birhauser, Boston.(1993)

[6] Buzsaki,G.,Two stage memory model: a role for noisy brain states, Neuroscience 31(3),551-570(1989)

[7] Buzsaki,G.,Hippocampal sharp wave-ripple: a cognitive biomarker for episodic memory and planning, Hippocampus Oct 25 (10),1073-1085,(2015)

[8] Colgin,L.,et a.,Frequency of gamma oscillations routes flow of information in the hippocampus. Nature, 462, 353-357,(2009)

[9] De Gannaro,L.,Ferrara,M.,Sleep Spindles: an Overview, Sleep Med Rev Oct 7(5) 423-40,(2003)

[10] Curto,C.,What can topology tell us about the neural code?,Bulletin of the AMS,54,63-78,(2017)

[11] Lopez da Silva,F.H.,Neural mechanisms underlying brain waves; from membranes to networks. Electroencephalography and Clinical Neurophysiology,79:81-93,(1991)

[12] Lopez da-Silva,F.,EEG: Origin and Measurements, in EEG-fMRI, Springer Verlag Berlin Heidelberg(2010)

[13] Dharani,K.,Biology of Thought, Academic Press,109-122,(2015)

[14] Fingelkurts,Andrew.,Fingelkuts,Alexander.,EEG Oscillatory States: Universality,Uniqueness and Specificity across Healthy-Normal, Alterted and Pathological Brain Conditions, PLOS One9(2),e87507,(2014)

[15] Heimburg, T., Jackson, A., On Soliton Propagation in biomembranes and nerves, PNAS, doi:10.1073/pnas.0503823102 (2005).

[16] Kanari.l,Dlotka.P,Scolamiero.M,Levi.R,Hess.K,Markram,H.,A topological representation of branching neuronal morphologies,Neuroinformatics16,3-13,(2018)

[17] Ioannides,A.,Liu,L.,Kostopoulos,G.,The Emergence of Spindles and K-complexes and the role of the Dorsal Caudal partof the Anterior Cingulate as the generator of K-complexes.,Frontiers of Neuroscience.,doi.org/10.3389/fnins.2019.00814

[18] Hong,S.,Dopamine System manager of neural pathways, Frontiers of Neuroscience v7 PMID 24367324,(2013)

[19] Jackson,J.D.,Classical Electrodynamics,191,Wiley and Sons,Inc(1962)

[20] Jones,S.,et al.,Neural mechanism of transient neocortical beta hythms: converging evidence from humans, computational modeling, monkeys and

mice. PNAS:16041351113,(2016)

[21] Kalla,C., Breathers and generalized non-linear Schroedinger equations as degenerations of algebro-geometric solutions, J.Phys.A: Math.Theor.44 (2011)

[22] Klimeschi,W. (2018) The frequency architecture of brain and brain-body oscillations: an analysis, Eu.J.Neuroscience 48(7),2431-2453

[23] Kalinchuk,A.,McCarley,R.,Porkka-Heiskanen,T.,Basheer,R.,Sleep Deprivation Triggers Inducible Nitric Oxide-Dependent Nitric Oxide Production in Wake-Active Basal Forbrain Neurons, The Journal of Neuroscience,30(40):13254-13264,(2010)

[24] Kitaev,A.,Notes on SL(2,R) representations, arXiv:1711.08169v2,(2018)

[25] Kim,Yoo Sung.,Choi,J.,Yoon,Bo-Eun.,Neuron-Glial Interactions in Neurodevelopment Disorder, Cell,Oct,9(10),2176,(2020)

[26] Liu,Ning-Han., Recognizing the Degree of Human Attention using EEG Signals for Mobile Sensors, Sensor(Basel)Aug, 10273-10286,(2013)

[27] Maier,R.,Associated Legendre Functions and Spherical Harmonics of Fractal Degree and Order; arXiv:1702.0855v3[math.CA],(2018)

[28] Marcolli,M.,Gamma Spaces and Information,J.Geometric Physics,140,26-55,(2019)

[29] Maya Geva-Sagiv, Yuval Nir.,Local Sleep Oscillations: Implications for Memory Consolidation, Frontiers Nueroscience,13,813,(2019)

[30] Miller,W.,The Lie theory approach to Special Functions. University of Minnesta, November,(2010)

[31] Morse,P and Feshbach, H Methods of Mathematical Physics,791, Chapter7, McGraw-Hill,(1953)

[32] Mumford,D.,Theta characteristics of an algebraic curve.,Ann.Scientifique del'Ecole Normale Superieure, Quatrieme, Series,4,181-192,(1971)

[33] Mumford,D.,Tata Lectures onTheta,Chapter1,3(1987)

[34] Nash,C.,Sen,S.,Topology and Geometry for Physicists, Academic Press,(1983)

[35] Munkres, J., Introduction to Topology, Chapter 12, Prentice Hall International Edition (2014)

[36] Nunez,P.L.,The Neurophysics of EEG(2006a) Second Edition, Oxford University Press

[37] Nunez,P.L and Srinivasan.,A theoretical basis for standing and traveling brain waves measured with human EEG with implications for integrated consciousness. Clinc Neurophysiol, 117(11),2424-2435,(2006b)

[38] Tomofumi Oga, et al.,Basal Dendrites of Layer 3, pyramidal neurons do not scale with change in cortical magnification in Macaque Primary Visual Cortex, (Fig 7), Frontiers Neuron Circuittes 10:74,(2016)

[39] Queenan,B., Ryan, T., Gazzanega, M., Gallistel, C., On the research of time past:The hunt for the substrate of memory, Annals of the New York Academy of Sciences, 1396, 108-125 (2017).

[40] Reimann,M.,Nolte.M,Scolamiero.M,Turner.K,Markram,H.,Cliques-of neurons bound into Cavities Provide a Missing Link between Structure

and Function,Frontiers in Computational Neuroscience,Vol 11,art 48(6 pages)(2017)

[41] Ronveaux,A.(Editor)(1995) Heun's Differential Equation, Oxford University Press

[42] Schwarz,H., Crelle Journal,75, 292-335,(1873)

[43] Scott,A.,Neuroscience, A Mathematical Primer, Springer,(2002)

[44] Sen,S.,Ryan,T.,Muldowney,D.,Pezzoli,M.,Memory as a Topological Structure on a Surface Network (submitted, 2021).

[45] Shrivastava, S., Schneider, M., Evidence for two-dimensional solitary sound waves in a lipid controlled interface and its implications for biological signalling, The Royal Society Interface, Vol 11, Issue 97 (2014).

[46] Suradi,Y.,Sawtooth waves, Neurology;84,e87-e88,(2015)

[47] Vidunas,R.,Transformation of algebraic Gaussian functions; arXiv-087.4808 [mathC.A](2008)

[48] Vidunas,R.,Funkcidaj Ekvacioj,139-180,(2009)

[49] Weigenand,A.,Shellenberger-Costa,M.,Ngo,Hong-Viet,V.,Claussen,J.C.,Characterization of K-complexes and Slow Wave Activity in a Neural Mass Model, PLOS Computational Biology, Nov 13 (2014)

[50] Wolfram MathWorld, Spherical Triangles

[51] Yoshida,M.,Fuchsian-Differential-Equations,Friedr.Vieweg-and-Sohn,(1987)

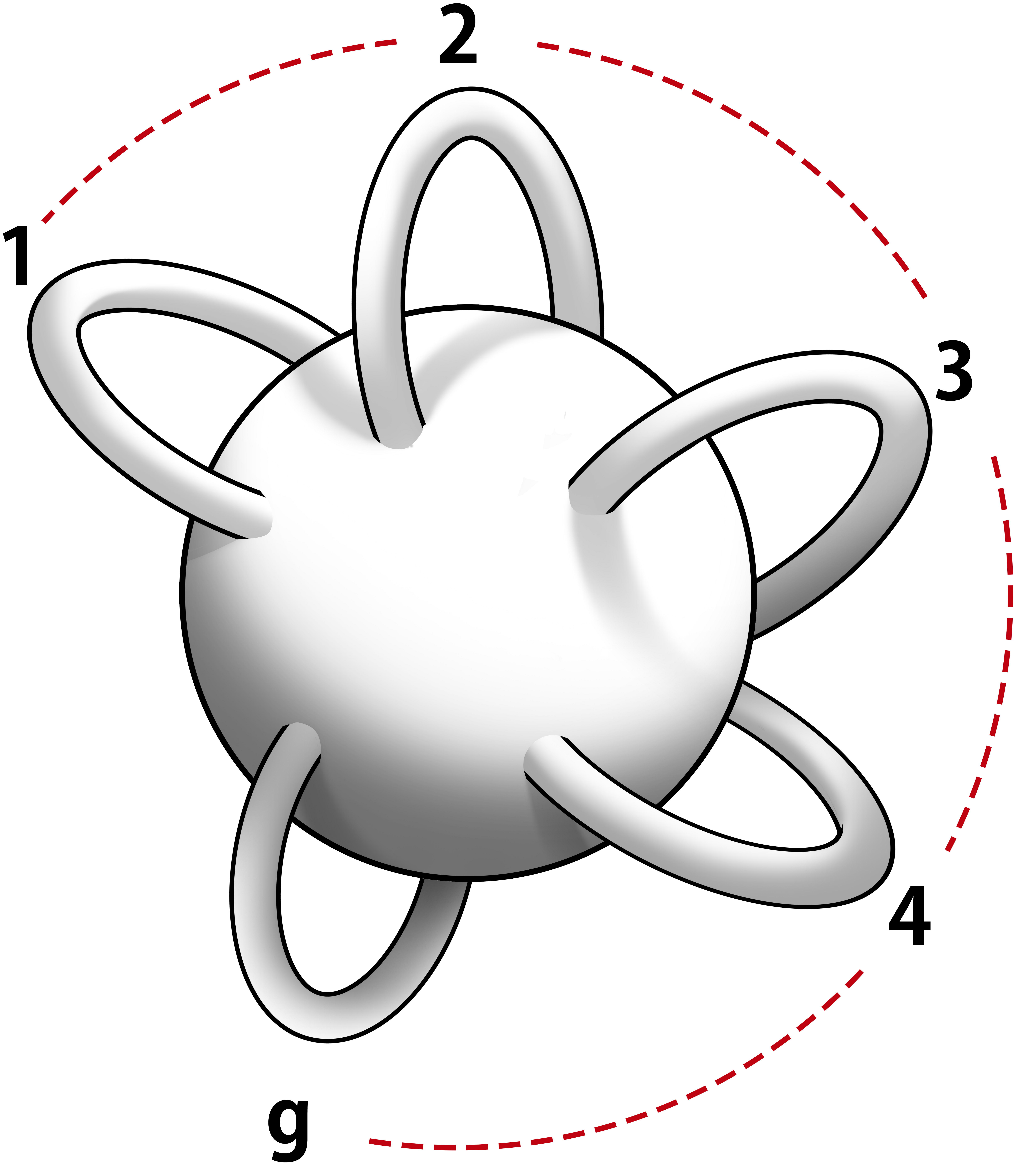
g

$b_1$
$b_2$
$b_3$
$b_g$
$a_1$
$a_2$
$a_3$
$a_g$

$a_1$
$a_2$
$a_3$
$a_j$

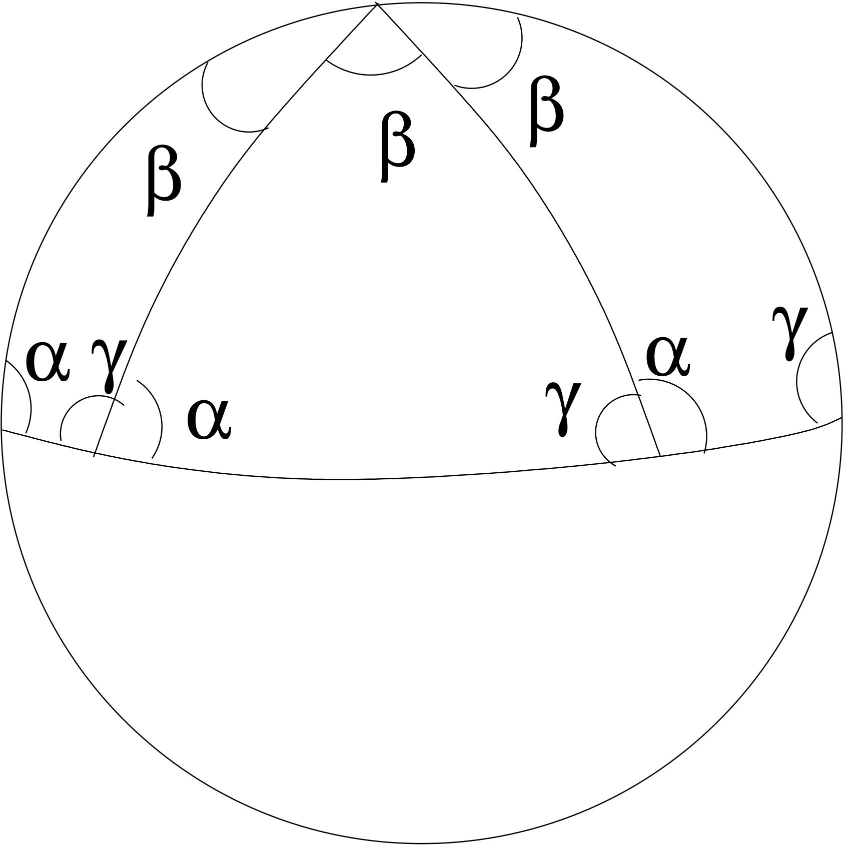
β
β
β
α
γ
α
γ
α
γ
α
γ

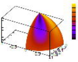
0.4
0
0.2
0.4
0.6
0.8
1
0
1

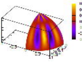
0.6
0.4
0.2
0
-0.2
-0.4
-0.6
1
0
0.5
1

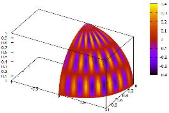

1
0.9
0.8
0.7
0.6
0.5
0.4
0.3
0.2
0.1
0
-1
-0.5
0
0.5
1
0
0.2
0.4
0.6
0.8
1
0.4
0.3
0.2
0.1
0
-0.1
-0.2
-0.3
-0.4

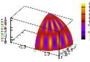
1
0
0.5
0.4
0.3

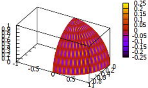
1
0.9
0.8
0.7
0.6
0.5
0.4
0.3
0.2
0.1
0
-1
-0.5
0
0.5
1
1
0.8
0.6
0.4
0.2
0
0.25
0.2
0.15
0.1
0.05
0
-0.05
-0.1
-0.15
-0.2
-0.25

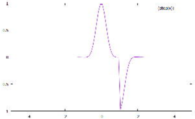
(stepx(x))
1
0.5
0
0.5
1
4
2
0
2
4

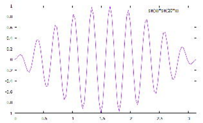
sin(x)*sin(20*x)
1
0.8
0.6
0.4
0.2
0
-0.2
-0.4
-0.6
-0.8
-1
0
0.5
1
1.5
2
2.5
3

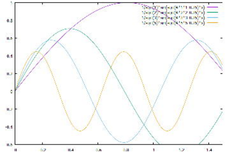
1/sqrt(1)*sin(sqrt(4*1*1 0.05)*x)
1/sqrt(2)*sin(sqrt(4*2*2 0.05)*x)
1/sqrt(3)*sin(sqrt(4*3*3 0.05)*x)
1/sqrt(5)*sin(sqrt(4*5*5 0.05)*x)
1
0.8
0.6
0.4
0.2
0
-0.2
-0.4
-0.6
0
0.2
0.4
0.6
0.8
1
1.2
1.4